



## **Radiative recombination mechanisms in aluminum tris(8-hydroxyquinoline): Evidence for triplet exciton recombination**

Curry, RJ; Gillin, WP

For additional information about this publication click this link.

<http://qmro.qmul.ac.uk/jspui/handle/123456789/4079>

Information about this research object was correct at the time of download; we occasionally make corrections to records, please therefore check the published record when citing. For more information contact [scholarlycommunications@qmul.ac.uk](mailto:scholarlycommunications@qmul.ac.uk)

# Radiative recombination mechanisms in aluminum *tris*(8-hydroxyquinoline): Evidence for triplet exciton recombination

R. J. Curry<sup>a)</sup> and W. P. Gillin

*Department of Physics, Queen Mary and Westfield College, University of London, London E1 4NS, United Kingdom*

(Received 29 November 1999; accepted for publication 12 April 2000)

The photoluminescence of aluminum *tris*(8-hydroxyquinoline) (AIQ) has been studied as a function of temperature and excitation wavelength. It was found that as the temperature and excitation energy is reduced the peak of the photoluminescence moves to longer wavelengths and broadens significantly. The photoluminescence spectra obtained at all temperatures and excitation energies can be deconvolved into three distinct peaks originating from three levels within the molecule. A rate-equation approach has been used to model the observed behavior and to obtain the relative lifetimes of the three processes responsible for the photoluminescence. From this we infer that at low temperatures and excitation energies the radiative recombination of triplet excitons is responsible for a significant amount of the photoluminescence of AIQ. It is this process which is responsible for the low energy tail seen in the photoluminescence of AIQ but which is not present in the electroluminescence. © 2000 American Institute of Physics. [S0021-8979(00)06614-7]

## I. INTRODUCTION

Aluminum *tris*(8-hydroxyquinoline) (AIQ) is one of the most extensively used molecules in organic light emitting diodes (OLEDs). It was first used by Tang and VanSlyke<sup>1</sup> as the electron transporting and emitting layer in an OLED along with N,N'-diphenyl-N,N'-bis(3-methylphenyl)-1,1'-biphenyl-3,3'-diamine (TPD) as the hole transporting material. In these OLEDs broad electroluminescence was obtained from the AIQ which peaked at 550 nm. Later OLEDs fabricated by VanSlyke *et al.*<sup>2</sup> in which a naphthyl-substituted benzidine derivative (NPB) was used as the hole transporting layer and AIQ as the emitting and electron transporting layer showed electroluminescence peaking at 528 nm. Further work on AIQ/TPD based OLEDs by Kalinowski *et al.*<sup>3</sup> reported electroluminescence emission from AIQ peaking at 520 nm. This work also noted that while the photoluminescence of AIQ also peaked at this wavelength there was more emission in the low energy tail of the photoluminescence compared to that of the electroluminescence.

Despite much work being carried out on the electrical properties of AIQ there has been little research into these differences in the reported electroluminescence of AIQ. The difference in the low energy tails of the photoluminescence and electroluminescence spectra of AIQ have previously been explained by the presence of "defect states" in the AIQ without any indication of the origin of these states.

In the work presented here we give a detailed examination of the photoluminescence AIQ as a function of excitation wavelength and temperature. We then use a rate-equation model approach to explain the observed results, from which some conclusions are drawn.

## II. EXPERIMENT

To obtain the photoluminescence a small quantity of bulk AIQ powder, as obtained from Alderich with a stated purity of 99.995%, was packed into a quartz cuvette. The sample was then placed into a continuous flow cryostat, the temperature of which could be controlled between 4 and 300 K. The excitation wavelengths used to obtain the photoluminescence were the 363, 457, 465, 476, and 488 nm lines of an argon ion laser with power densities of 10, 100, 10, 15, and 100 mW, respectively. The photoluminescence was then dispersed in a 1 m spectrometer, with a 1200 line/mm grating blazed at 500 nm, before being detected using a S-20 photomultiplier tube. The resolution of the system was 0.8 nm for all of the spectra collected.

To obtain the electroluminescence of AIQ, an indium tin oxide (ITO)/TPD (400 Å)/AIQ (500 Å)/Al (2000 Å) OLED was fabricated. The OLED was then placed into the cryostat and the electroluminescence was obtained using the same system as used to collect the photoluminescence. All spectra were corrected for the response of the system.

## III. RESULTS

Figure 1 (top) shows the photoluminescence of AIQ obtained using the 363 nm excitation wavelength at 25 and 300 K along with the electroluminescence obtained from the AIQ based OLED. It can be seen that with the reduction in temperature there is a corresponding fall in the photoluminescence intensity. Accompanying this reduction in intensity is a movement of the photoluminescence peak from 510 to 504 nm and a reduction in the full width at half maximum (FWHM) from 436 to 422 meV at 300 and 25 K, respectively. This reduction in the FWHM with temperature is what would normally be expected if phonon interactions

<sup>a)</sup>Electronic mail: r.j.curry@qmw.ac.uk

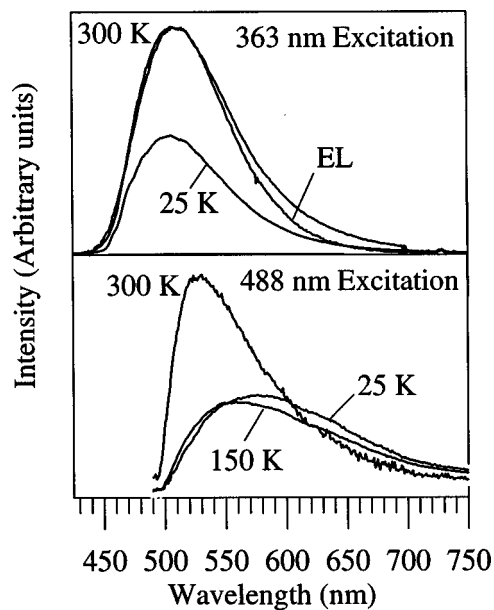


FIG. 1. The photoluminescence of AIQ obtained using the 363 (top) and 488 nm (bottom) excitation wavelengths at selected temperatures. Shown for comparison is the electroluminescence of a ITO/TPD/AIQ/Al OLED (top).

were thought to be responsible for the broad spectra at room temperature.

Also shown in Fig. 1 (top) is the 300 K electroluminescence spectra obtained from the AIQ based OLED. It can be seen that the peak and high energy tail of the electroluminescence is almost identical to the 363 nm excited photoluminescence obtained at the same temperature. In contrast to this, the low energy tails of these two spectra are very different with the photoluminescence containing appreciably more emission at longer wavelengths.

Figure 1 (bottom) shows the 488 nm excited photoluminescence obtained at 300, 150, and 25 K. The effect of reducing the temperature, for this excitation wavelength, is the opposite to that observed when using the 363 nm excitation. The peak position of the photoluminescence increases from 530 to 577 nm as the temperature is reduced from 300 to 25 K corresponding to a shift of 190 meV towards lower energies. With this shift, there is also a large increase in the FWHM from 369 meV at 300 K to 562 meV at 25 K. Furthermore, careful inspection of the photoluminescence spectrum obtained at 25 K shows the presence of a second peak centred at  $\sim 620$  nm.

The effect of reducing the temperature, on the photoluminescence obtained using the other excitation wavelengths, was similar to that seen for the 488 nm excited photoluminescence. Figure 2 shows a summary of the movement of the photoluminescence peak position, in electron volts, as a function of excitation wavelength and temperature. It can be seen that the peak position of the 363 nm excited photoluminescence increases by 30 meV from 2.43 to 2.46 eV as the temperature is reduced. In contrast to this, for all other excitation wavelengths, there is a decrease in the photoluminescence peak position with temperature. The shifts towards a lower energy are 40, 80, 90, and 190 meV for the 457, 465, 476, and 488 nm excitation wavelengths, respectively.

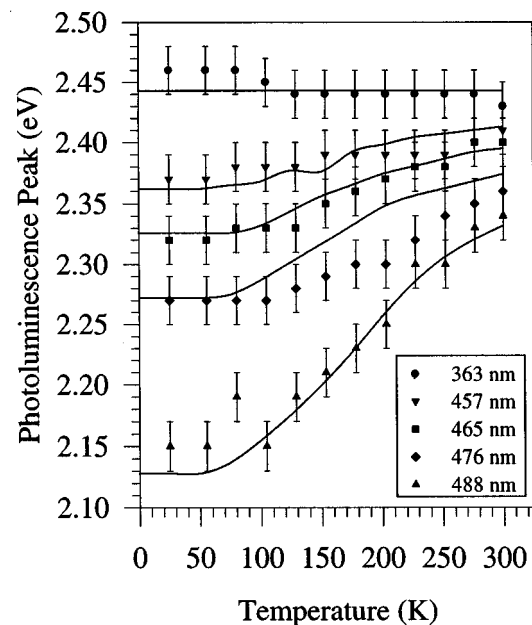


FIG. 2. The peak position of the photoluminescence of AIQ as a function of temperature and excitation wavelength. The solid lines are the predicted movement in peak position obtained from the rate-equation model.

476, and 488 nm excitation wavelengths, respectively. From this figure it can also be seen that most of the movement in peak position occurs at temperatures above 125 K and below this temperature there is little further movement.

#### IV. DECONVOLUTION OF PHOTOLUMINESCENCE

First, we attempted to deconvolve the photoluminescence spectra obtained at 25 K, using the 457, 465, and 476 nm excitations, into the two spectra obtained using the 363 and 488 nm excitations at the same temperature. While we could get a fit of the peak positions for each spectra using this method, the shape of the spectra was not a good fit. This is not surprising given that the 25 K 488 nm excited photoluminescence can be seen to have two components. We therefore used three peaks in the deconvolution and found that we could deconvolve all of the spectra obtained at each temperature to a high degree of accuracy. Figure 3 shows the deconvolution of the 476 nm excited photoluminescence along with the three peaks used weighted appropriately. The variation in the high energy tail between the fit and the spectra is due to the color glass filters used when collecting the spectra to protect the detector from the laser. The position of the three peaks was found to be nonarbitrary; a movement of as little as 20 meV in the peak position of any of the three peaks was found to seriously effect the quality of the fit. Using these three peaks it is possible to accurately deconvolve the photoluminescence of AIQ obtained for all excitation wavelengths and temperatures. These three peaks then can be used to provide a unique description of the photoluminescence recombination in AIQ.

The three peaks used in the deconvolution were polynomials. Peak 1 in Fig. 3 is a polynomial fitted to the electroluminescence spectra obtained from the AIQ based OLED.

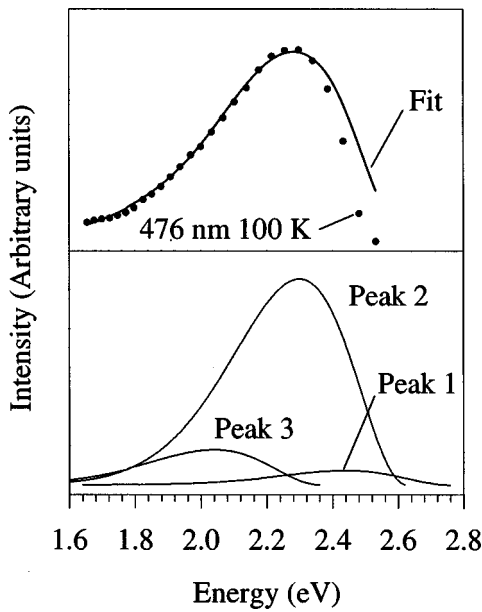


FIG. 3. The fit obtained to the 476 nm excited photoluminescence at 100 K (top) using peaks 1–3 weighted as shown (bottom).

This was used as it appears only to contain emission from the high energy level unlike the 363 nm excited photoluminescence, which contains emission from all three levels. This would account for the observed differences between the tails of the photoluminescence and electroluminescence spectra. For peaks two and three the same polynomial, shifted to lower energies was used. This approach assumed that the emission from these other levels has the same shape and width as peak 1, and the quality of the fits shows that this assumption is not unreasonable. The positions of the three peaks are 2.45, 2.30, and 2.04 eV each of them having a FWHM of 420 meV. The position of peak 3 also coincides with the second peak seen at  $\sim 620$  nm (2 eV) in the 488 nm excited photoluminescence at 25 K. While the fits obtained using these three peaks are very good it may be possible to make slight improvements by varying the widths of the three peaks. While it is not unreasonable that peaks 2 and 3 do have different widths, any large changes of these widths would lead to decrease in the quality of the fits obtained.

Figure 4 shows the weighting of the three peaks when fitting the photoluminescence obtained at 25 K. This plot gives an effective photoluminescence excitation spectrum for AIQ. It can be clearly seen that at excitation wavelengths below 450 nm most of the absorption, which then results in emission, occurs into the high energy level. As the excitation wavelength is increased however this absorption switches into the lower energy levels. The inset to Fig. 4 shows the absorption spectra for AIQ. It should be noted that the excitation wavelengths used are in the extreme tail of the absorption spectrum of AIQ and so are only weakly absorbed.

**V. MODELING OF RESULTS**

The deconvolution shows that the photoluminescence spectra of AIQ at all temperatures and for all excitation wavelengths can be described by assuming emission from

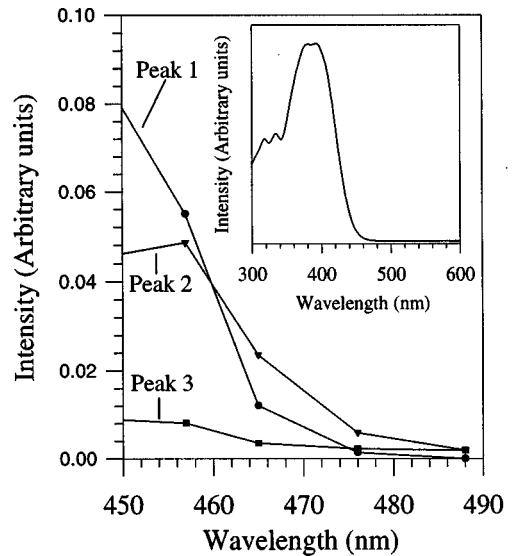


FIG. 4. The weighting factors of peaks 1–3 used when fitting the photoluminescence spectra obtained at 25 K. The lines continue on to the weighting factors used to fit the 363 nm excited photoluminescence. The inset shows the absorption spectra of AIQ in solution.

just three levels, with some apparent thermally activated transfer of excitons between these levels. We have therefore used a rate-equation approach to model the observed changes in the photoluminescence with temperature and excitation wavelength, in order to try and gain some insight into the processes occurring. Figure 5 shows a schematic of the model used where  $m_1$ ,  $m_2$ , and  $m_3$  represent the three states responsible for the luminescence. Each of these levels is fed by a pump, the rate of which is a function of excitation wavelength only and not temperature. This model makes the assumption that none of the energy levels either shifts or broadens in energy as the temperature is raised, and that the effective absorption into each of these levels is constant with temperature. Exciton transfer between the levels is allowed but is limited by a thermal energy barrier between the different levels. The final photoluminescence peak is then the sum

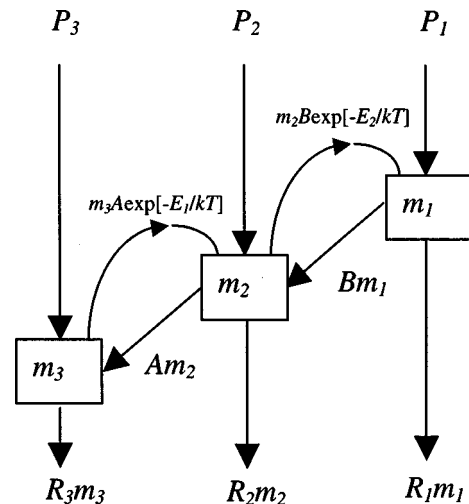


FIG. 5. Schematic of the rate-equation scheme used to model the photoluminescence dependence on temperature and excitation wavelength.

of the emission from each of the three levels, which are determined by the population in a level and the recombination rate for that level. At low temperatures there will only be transfer of excitons from a high energy level to a low energy level due to the presence of the thermal barrier. As the temperature is increased, however, transfer will be able to take place from a low energy level to a higher energy level through thermally assisted tunnelling or by interacting with phonons. If the recombination time of a high energy level is shorter than that of a lower energy level then the resulting spectra, obtained by adding the output from each of the three levels, will move towards that of the high energy level as the temperature is increased.

In the rate-equation scheme shown in Fig. 5,  $P_i$  is the pump rate into each of the levels,  $i$ , with an independent population  $m_i$ . The rate constant for the transfer of an exciton from a lower energy level to a higher energy level takes the form

$$\text{Transfer Rate} = A \exp\left[-\frac{E_i}{kT}\right], \quad (1)$$

where  $E_i$  is the thermal energy barrier between the two levels,  $k$  is Boltzmann's constant, and  $T$  is the temperature. The transfer rate constant for the opposite transfer is then  $A$ . The rate constant for radiative recombination from each level is given by  $R_i$ . To describe the system in steady state the rate equations are

$$\frac{dm_1}{dt} = 0 = P_1 + m_2 B \exp\left[-\frac{E_2}{kT}\right] - m_1 B - m_1 R_1 \quad (2)$$

$$\begin{aligned} \frac{dm_2}{dt} = 0 = P_2 + m_1 B + m_3 A \exp\left[-\frac{E_1}{kT}\right] - m_2 B \\ \times \exp\left[-\frac{E_2}{kT}\right] - m_2 A - m_2 R_2 \end{aligned} \quad (3)$$

$$\frac{dm_3}{dt} = 0 = P_3 + m_2 A - m_3 A \exp\left[-\frac{E_1}{kT}\right] - m_3 R_3, \quad (4)$$

and the photoluminescence intensity from each level is given by

$$I_i = R_i m_i. \quad (5)$$

These three simultaneous equations [Eqs. (2)–(4)] can be solved for  $m_i$  giving an expression for the photoluminescence intensity from each level in terms of the model parameters. The pump rates,  $P_i$ , were taken to be the weights of peaks 1–3 used when fitting the photoluminescence at 25 K which give an effective photoluminescence excitation spectrum, Fig. 4.

Values were then assigned for the other parameters in the model and for each temperature and excitation wavelength the predicted output intensity of each level was obtained. Peaks 1–3 were then multiplied by their corresponding output intensity,  $I_i$ , obtained from the model. The three peaks were then added and the peak position of the resulting spectra was compared to that of the experimentally observed spectra. Using a process of trial and error the parameters of the model were varied until the predicted change in the peak

TABLE I. The values of the parameters used in the rate-equation model shown schematically in Fig. 5. The errors on the rate terms are  $<50\%$ .

Parameter	Value	Parameter	Value
$E_1$	$6 \pm 2$ meV	$R_1$	$>100\,000 \leq 50\%$
$E_2$	$11 < \pm 4$ meV	$R_2$	$40 < \pm 50\%$
$A$	$0.8 < \pm 50\%$	$R_3$	$0.8 < \pm 50\%$
$B$	$80 < \pm 50\%$		

position of the photoluminescence with excitation energy and temperature was a good fit of the observed data. The solid lines in Fig. 2 show the peak position of the photoluminescence as predicted by the model for each temperature and excitation along with the experimental data. The values of the fitting parameters used to obtain this fit are given in Table I.

It should be noted that, when using the rate-equation model, the aim was to attempt to fit all of the data with a trend and not just one spectra, as in Fig. 3. As a result, the predicted photoluminescence spectra from the model will not always be a perfect fit to the experimental spectra obtained for a given excitation wavelength and temperature. In spite of this it was found that only in a few cases did the predicted spectra shape vary significantly from the experimentally obtained spectra.

Given the excellent agreement between the model and the experimental data it is important to question the ‘‘accuracy’’ of the fitting parameters. The values of the activation energies in the model are primarily determined by the temperatures at which transfer is seen to occur between the levels. For  $E_1$  where there is a large change in the 488 nm excited photoluminescence this significantly limits the error in  $E_1$  to the order of  $\pm 2$  meV. For  $E_2$  the transition from level 2 to level 1 can be less easily seen but significant changes to  $E_2$  results in the quality of the overall fit being significantly reduced. Using this as guide it is reasonable to say that the error in  $E_2$  is of the order of  $< \pm 4$  meV. Given these constraints upon the fitting it was found that the rate terms are limited to an error of  $<50\%$ .

## VI. DISCUSSION AND CONCLUSION

While this model is successful in predicting the temperature dependence of the photoluminescence for a given wavelength further work is needed to fully understand the origin of these levels. However, there are some physical conclusions that can be drawn from the model. Level 1 is almost certainly the singlet recombination and this is supported by the small recombination lifetime inferred from the large value of  $R_1$  in the model. The rate term for this level is at least three orders of magnitude faster than the rate for level 2 which in turn is about an order of magnitude faster than level 3. Similarly, we can state that the rate terms for transfer between these levels is of the same order as the radiative rate out of these levels. Finally, we can state that the thermal energy required for transfer between the levels is very small and it is the low probability of these events which limit them.

While we do not know the exact origin of the lower energy levels we suggest that they could be due to optical



emission from the triplet states. This direct recombination of a triplet can occur if there is a suitable perturbation (e.g., spin-orbit interactions) but would have a low probability, which is reflected in the low rate terms in the model. More interestingly, this model gives some feel for the probability of transfer between triplet states and between triplet and singlet states.

This would suggest that the low energy tail in the photoluminescence spectra of AIQ is due to the recombination of triplets, unlike as some workers have suggested,<sup>3-5</sup> defect states within AIQ. Given that this tail is not as prominent in the electroluminescence then this further implies that there is very little emission from triplet recombination processes in the electroluminescence of these OLEDs. One reason for this may be related to the electroluminescence emission originating from very thin films,  $\sim 50$  nm, unlike the

bulk powder used to obtain the photoluminescence. Given the long recombination lifetime of the triplet states the probability of nonradiative recombination maybe greatly increased by the presence of interface states. While we could not obtain direct lifetime measurements of the photoluminescence from the low energy tail, such measurements should give the radiative recombination lifetime for triplet excitons in AIQ.

<sup>1</sup>C. W. Tang and S. A. VanSlyke, *Appl. Phys. Lett.* **51**, 913 (1987).

<sup>2</sup>S. A. Vanslyke, C. H. Chen, and C. W. Tang, *Appl. Phys. Lett.* **69**, 2160 (1996).

<sup>3</sup>J. Kalinowski, N. Camaioni, P. Di Marco, V. Fattori, and G. Giro, *Int. J. Electron.* **81**, 377 (1996).

<sup>4</sup>T. Mori, S. Miyake, and T. Mizutani, *Jpn. J. Appl. Phys., Part 1* **34**, 4120 (1995).

<sup>5</sup>E. W. Forsythe, D. C. Morton, C. W. Tang, and Y. Gao, *Appl. Phys. Lett.* **73**, 1457 (1998).